J Mater Sci (2006) 41:6300–6304
DOI 10.1007/s10853-006-0336-9

Sinterable $La_{0.8}Sr_{0.2}CrO_3$ and $La_{0.7}Ca_{0.3}CrO_3$ powders by sucrose combustion synthesis

K. Prabhakaran · J. Lakra · M. O. Beigh · N. M. Gokhale · S. C. Sharma · Ramji Lal

Received: 1 July 2004 / Accepted: 18 August 2005 / Published online: 12 August 2006

Abstract Air atmosphere sinterable $La_{0.8}Sr_{0.2}CrO_3$ [LSC] and $La_{0.7}Ca_{0.3}CrO_3$ [LCC] powders have been prepared by sucrose combustion synthesis. Aqueous solution containing stoichiometric quantities of the metal nitrates and sucrose (3 moles/mole of the metal ion) at pH ~1 was concentrated by heating on a hot plate into a viscous resin which on drying at 120 °C produced a foam with interconnected pore structure. This foam ignited with a matchstick in a combustion set up fabricated in the laboratory produced ashes consisting of loose aggregate of LSC and LCC particles. The loose aggregates of LSC and LCC were powdered by planetary ball milling to submicron size particles with D_{50} value 0.19 and 0.60 μm, respectively. The surface area of the LSC and LCC powders was 23 and 19 m^2/g, respectively. Pellets prepared by cold compaction and sintering of LSC and LCC powders in air atmosphere showed density 96.8 and 98.8% of theoretical value respectively. Sintered LCC sample showed finer grains compared to the LSC sample under identical processing conditions.

Introduction

Doped lanthanum chromite [$La_{0.8}Sr_{0.2}CrO_3$ (LSC) and $La_{0.7}Ca_{0.3}CrO_3$ (LCC)] materials having high electronic and low ionic conductivity, as well as thermal stability in both oxidizing and reducing atmospheres, have been used as interconnect materials in solid oxide fuel cells (SOFCs) [1–3]. One inherent problem associated with these materials is their poor sinterability in air or oxidizing atmospheres [4–6]. This is due to volatilization of Cr as Cr_2O_3 above 1000 °C which forms a thin layer of Cr_2O_3 at the inter particle neck during the initial stages of sintering. However, the density of interconnect material should be near to the theoretical value to prevent intermixing of oxygen and fuel in the solid oxide fuel cell stack. Several attempts have been made to increase the sinterability of lanthanum chromite. These have included the preparation of highly reactive fine powders, the introduction of chromium deficiencies, the substitution of chromium by dopants such as Al, Zn and Ni, the use of several sintering aids and the adoption of novel sintering techniques such as spark plasma sintering [7–10]. However, the addition of other elements degrades the chemical stability of these materials for long periods of operation of the SOFC at high temperatures [10, 11].

It is also clear that the sinterability of lanthanum chromite depends on the powder synthesis route [12]. Solid state synthesis, polymer precursor synthesis using citric acid and ethylene glycol, an emulsion process, spray pyrolysis and aqueous combustion synthesis using nitrate salts and glycine have been reported for lanthanum chromite [6, 12, 13–16]. Lanthanum chromite powders prepared by these methods sintered to 85–96% of the theoretical density (TD) at 1600 °C. Recently, sucrose has been used as a fuel for the combustion synthesis of ceramic oxide powders [17–20]. Previous studies on the combustion synthesis of lanthanum strontium manganite (LSM) using sucrose as a fuel showed the formation phase pure fine powders (D_{50} ~ 0.2 μm) with very good sinterability [21]. The present paper reports on the

K. Prabhakaran (✉) · J. Lakra · M. O. Beigh · N. M. Gokhale · S. C. Sharma · R. Lal
Naval Materials Research Laboratory, Shil-Badlapur Road, Anandnagar P.O. Addl. Ambernath, Thane 421 506, India
e-mail: kp2952002@yahoo.co.uk

preparation of LSC and LCC powders using the sucrose combustion method.

Experimental

Lanthanum nitrate (CDH, Delhi), strontium nitrate (Merck, India), chromium nitrate (Merck, India) and sucrose (Merck, India) used for this study were AR grade. Nitric acid (Merck India) was used for pH adjustments. Calcium nitrate was prepared by dissolving AR grade calcium carbonate (CDH, Delhi) in dilute nitric acid. Distilled water was used for the preparation of solutions.

The flow chart of the process is shown in Fig. 1. Sucrose and a stoichiometric amount of lanthanum nitrate, strontium nitrate or calcium nitrate and chromium nitrate were dissolved in the minimum quantity of water and the pH of the resulting solution was adjusted to 1.0 using nitric acid. The amount of sucrose used was three moles per mole of metal ion. This homogeneous solution was heated on a hot plate till it becomes a dark viscous resin, which was further dried in an air oven at 120 °C. The thermo gravimetric analysis (TGA) and differential thermal analysis (DTA) of the dried samples were carried out in air at a heating rate of 10 °C/min. using a thermal analyzer (Setsys 16/18, Setaram Scientific and Industrial Equipment, France).

The dried resin was ignited in a laboratory combustion set up made on site and the ignition was initiated with a match. Figure 2 shows a schematic diagram of the experimental combustion set up. It consists of a cylindrical

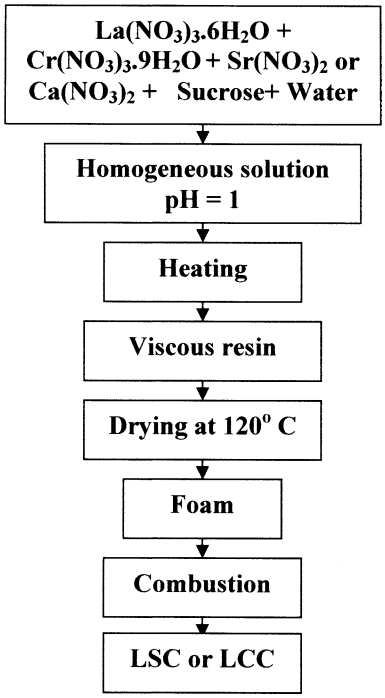

Fig. 1 Flow chart of the sucrose combustion process

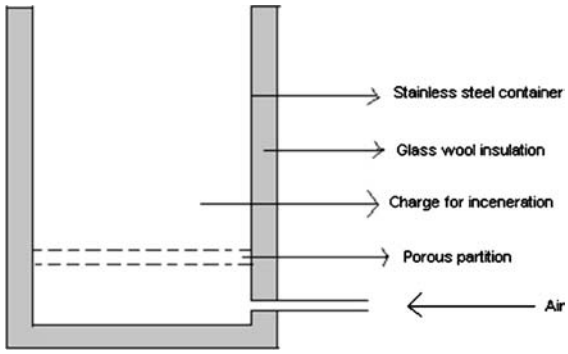

Fig. 2 Schematic diagram of the experimental combustion setup

stainless steel vessel, which is divided in to two compartments by means of a porous partition. The material for combustion is charged in the top compartment and air is passed from the lower compartment, through the porous partition. The walls of the vessel are insulated with glass wool mat to minimize heat loss. The ash obtained was analyzed using an X-ray diffractometer (Philips analytical PW 1710) with Cu Kα radiation. The crystallite sizes of the powders were calculated from X-ray diffraction (XRD) data using the Scherer equation. The combustion ash was deagglomerated by planetary ball milling in isopropanol medium for 24 h using zirconia grinding media. A charge to ball ratio of 1:4 by weight was used during milling. Particle size analyses of the powders were carried out using a Malvern Master Size analyzer 2000. The surface area of the powders was measured by Brunauer-Emmett-Teller (BET) method (Sorptomatic 1990, Thermo Fennigan). The powders were compacted by uniaxial pressing at 50 MPa pressure and sintered at various temperatures within the range 1450–1650 °C for 3 h. Densities of the sintered samples were measured by Archimedes principle using water. Microstructures of the ashes, deagglomerated powders and fracture surfaces of sintered samples were observed in a scanning electron microscope (LEO 1455).

Results and discussion

It is well known that when an aqueous acidic sucrose solution is concentrated by heating it forms a dark viscous resin due to polymerization of sucrose. The metal ions (La^{3+}, Cr^{3+} and Sr^{2+} or Ca^{2+}) present in the system are expected to interact with the sucrose polymer by co-ordination through the –OH groups which makes their homogeneous distribution possible throughout and prevents their segregation during drying. On drying, this resin undergoes foaming and the foam volume was found to be about 36 times the initial volume of the resin. Figure 3 shows the microstructure of a thin section of the foam observed using an optical microscope. The foam has open

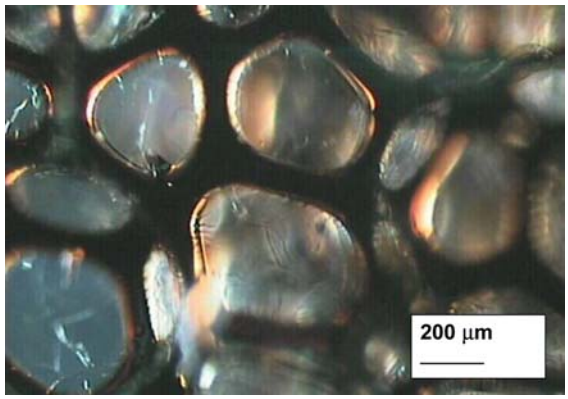

Fig. 3 Optical microstructure of a thin section of the foam obtained by heating aqueous La, Sr and Cr nitrate and sucrose

interconnected pores with sizes in the range 100–300 μm and the cell walls are only a few microns thick. This structure enables the foam to undergo easy combustion, like a dry cellulose material, when ignited.

Figure 4 shows the TGA–DTA plot of the dried foam sample. A weak exothermic peak observed in the temperature range 160–180 °C is due to the charring of sucrose polymer and the strong exothermic peak observed in the temperature range 300–380 °C is due to combustion of carbon by the nitrate oxidant present in the system. Weight loss from the foam sample is completed at 400 °C. As expected, the dried foam undergoes combustion with a strong flame when ignited with a match inside the set up shown in Fig. 2. The flame subsides in a few minutes leaving a red hot mixture of carbon and other inorganics. The slow combustion of carbon continued until all the carbon was removed from the system and the process took a maximum of one hour for a 100 g LSC or LCC batch. The temperature of the system rose to 725 °C during combustion as measured using an appropriate thermocouple setup. The glass wool insulation minimizes heat loss and maintains the temperature above 600 °C throughout the combustion process, which would be conducive for the desired phase formation. The LSC and LCC ashes obtained

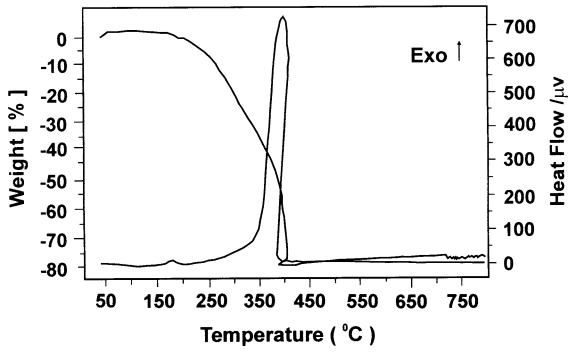

Fig. 4 TGA–DTA plot of a sample of the foam obtained by heating aqueous La, Sr and Cr nitrate and sucrose

showed a weight loss of 0.40 and 0.33 wt%, respectively when heated at 700 °C for 2 h indicating that the carbon burn out is apparently completed during the combustion process. Figure 5 shows XRD patterns of the LSC and LCC ashes. It is clear that perovskite LSC and LCC phases were formed during the combustion process. Figure 6 shows scanning electron microscopy (SEM) micrograph of LSC ash. The ash contains loose and porous aggregates of fine particles, which can be easily broken down in to primary particles by ball milling. The aggregates size varies from a few microns to 100 micron. A similar aggregate size and morphology were observed in SEM microstructures of LCC ash.

Figure 7 shows the particle size distribution of LSC and LCC powders obtained after planetary milling of the corresponding ashes. Both LSC and LCC powders showed narrow particle size distributions. The LSC powder has particle sizes in the range 0.12–0.32 μm with a D_{50} value of 0.19 μm. On the other hand, LCC powder particles are relatively larger in size being in the range 0.48–0.83 μm with a D_{50} value of 0.6 μm. The crystallite sizes calculated from XRD data using the Scherer equation were 14.4 and 13.9 nm for the LSC and LCC, respectively. Figure 8 shows the microstructure of the LSC powder. Both primary particles and particle agglomerates are seen in the figure.

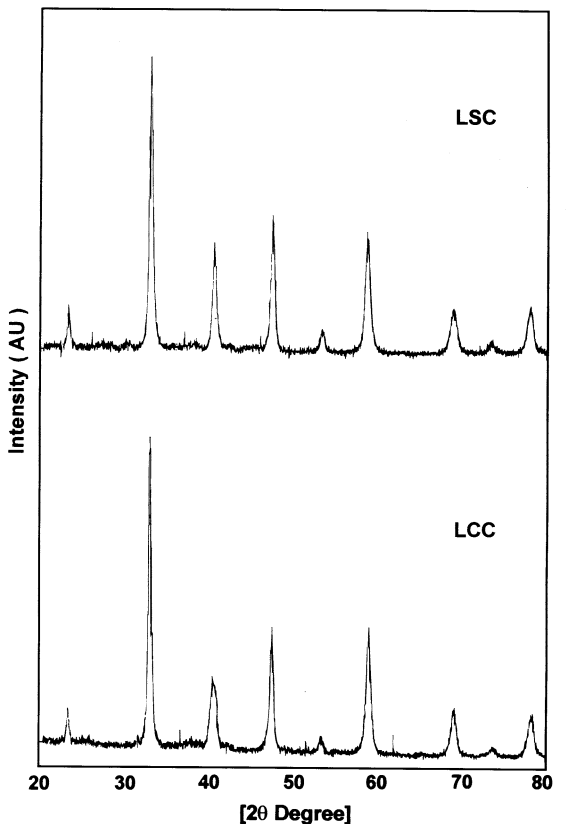

Fig. 5 XRD pattern of the ashes obtained by combustion of the foams

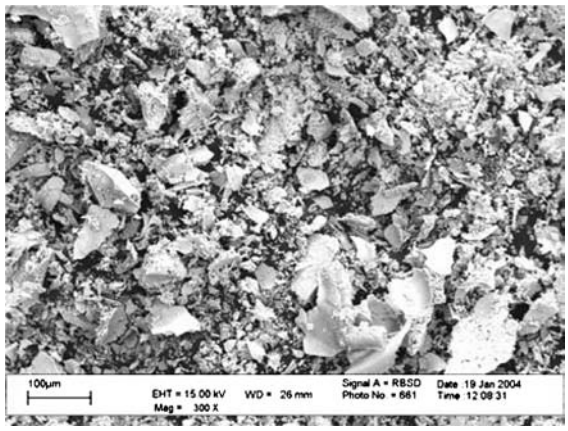

Fig. 6 SEM photomicrograph of the LSC ash

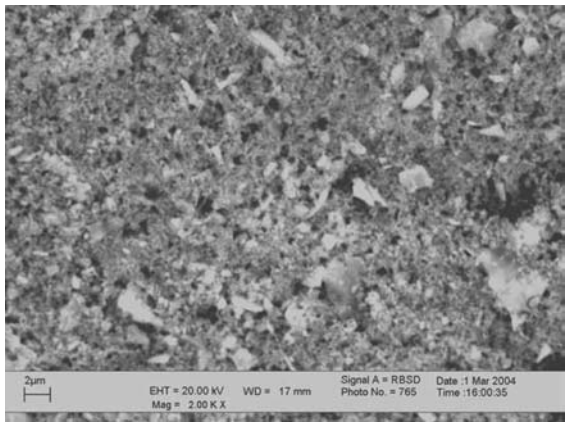

Fig. 8 SEM photomicrograph of the LSC powder

Similar features were observed in the SEM micrograph of LCC powder. The surface areas of the LSC and LCC powders were 23 and 19 m^2/g, respectively.

Figure 9 shows the variation of sintered density of the LSC and LCC powder compacts with sintering temperature. The percentage of theoretical density was calculated with respect to the theoretical density of LSC (6.57 g/cm^3) and LCC (6.06 g/cm^3) obtained from X-ray crystallographic data. LSC powder compacts sintered at 1450 °C were showed 83.5% TD as compared with 73.5% TD observed for LCC powder compacts sintered at the same temperature. Density value increased rapidly with sintering temperature for both the powders up to 1550 °C and then slowly up to 1600 °C. After 1600 °C there is no significant improvement in sintered density. The densities of the LSC and LCC powder compacts sintered at 1600 °C were 96.8 and 98.8% TD, respectively. The density values obtained are higher than those reported for the same compositions prepared by other methods. This shows that both the powders are reactive and sinter in an air atmosphere. The higher sintered density obtained for LSC at lower temperature is attributed to its fine powder particle size.

Figure 10 shows the microstructures of LSC and LCC samples sintered at 1600 °C for 3 h. Both LSC and LCC samples showed intragranular fracture with few grain pull outs. A very small number of micro pores were seen within the grains of the LSC sample, which is in agreement with its lower density compared with the LCC sample. The LCC sample had a smaller grain size compared with the LSC sample. Most of the grains in the LCC sample are below 1 µm and the maximum grain size observed was 2 µm. However, most of the grains in the LSC sample were in the size range 2–4 µm.

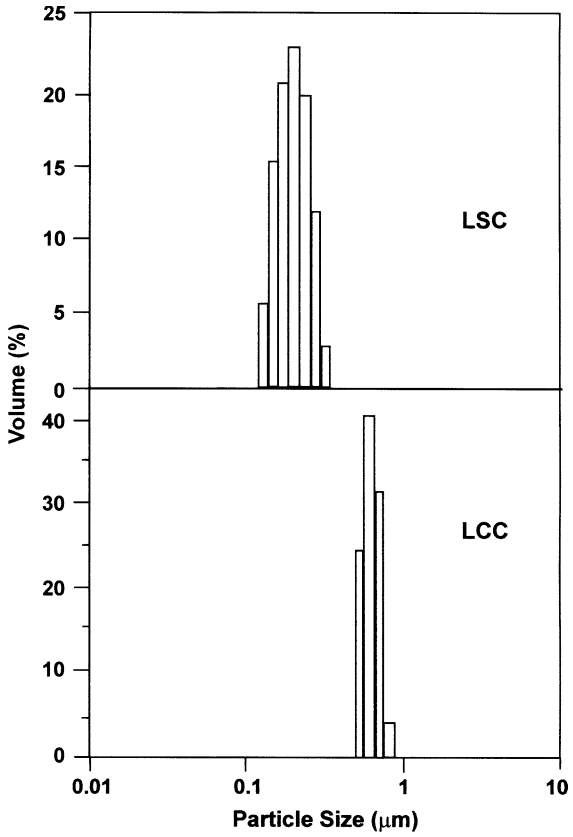

Fig. 7 Particle size distribution of the LSC and LCC powders

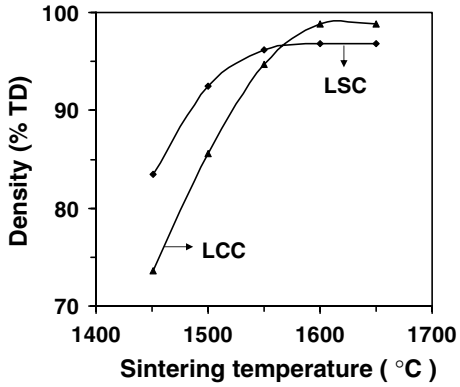

Fig. 9 Density of the LSC and LCC powder compacts sintered at various temperatures

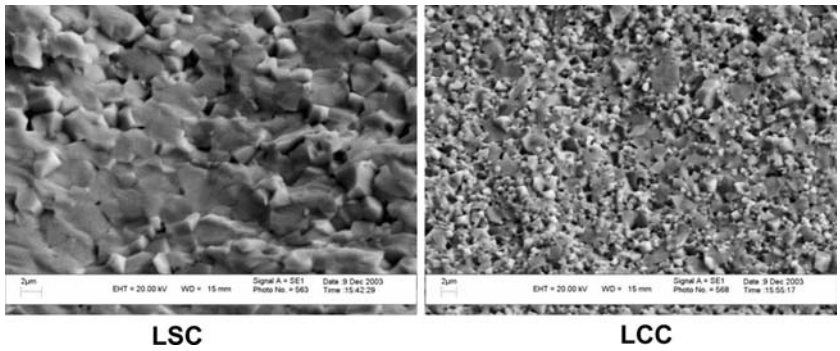

Fig. 10 SEM photomicrograph of fracture surface of the LSC and LCC samples sintered at 1600 °C for 3 h

Conclusions

Air atmosphere sinterable powders of LSC and LCC have been prepared using a sucrose combustion technique. LSC and LCC phases were formed during the self sustained combustion of the foams obtained from heating aqueous metal (La, Cr, and Sr or Ca) nitrates and sucrose. LSC and LCC powders obtained by planetary milling of the combustion ashes have surface areas of 23 and 19 m^2/g and contain submicron particles with D_{50} values of 0.19 and 0.6 μm, respectively. The LSC and LCC powder compacts sintered to 96.8 and 98.8% TD at 1600 °C. The sintered LCC sample had a smaller grain size compared with the LSC sample.

Acknowledgement The authors thank Dr. J. Narayana Das, Director, Naval Materials Research Laboratory for his encouragement and keen interest in this work.

References

1. Minh NQ (1993) J Am Ceram Soc 76:563
2. Steele BCH (2001) J Mater Sci 36:1053
3. Steele BCH (1992) Mater Sci Eng 1313:79
4. Chick LA, Liu J, Stevenson JW, Armstrong TR, Mc Cready DE, Maupin GD, Coffey GW, Coyle CA (1997) J Am Ceram Soc 80:2109
5. Groupp L, Anderson HU (1976) J Am Ceram Soc 59:447
6. Sakai N, Kavada T, Yokokawa H, Dokiya M (1990) J Mayter Sci 25:4531
7. Christie GM, Middleton PH, Steele BCH (1993) In Singhal SC, Iwahara H (eds) Proceedings of the 3rd international symposium on solid oxide fuel cells. The Electrochem. Soc., Pennington, NJ, p 315
8. Christiansen N, Gordes P, Alstrup NC, Mogensen G (1993) In Singhal SC, Iwahara H (eds) Proceedings of the 3rd international symposium on solid oxide fuel cells. The Electrochem. Soc., Pennington, NJ, p 401
9. Yokokawa H, Sasaki N, Kawada T, Dokiya M (1991) J Electrochem Soc 138:1018
10. Takeuchi T, Takeda Y, Funahashi R, Aihara T, Tahuchi M, Kageyama H (2000) J Electrochem Soc 147:3979
11. Christie GM, Middlton PH, Steele BCH (1994) J Euro Ceram Soc 14:163
12. Deshpande K, Mukasyan A, Varama A (2003) J Am Ceram Soc 86:1149
13. Weber WJ, Griffin CW, Bates JL (1987) J Am Ceram Soc 70:265
14. Eror NG, Anderson HU (1989) Mater Res Soc Symp Proc 73:571
15. Ovenstone J, Ponton CB (2000) J Mater Sci 35:4115
16. Vernoux P, Djurado E, Guillodo M (2001) J Am Ceram Soc 84:2289
17. Das RN, Bandyopadhyay A, Bose A (2001) J Am Ceram Soc 84:2421
18. Mitchell LD, Whitfield PS, Margeson J, Beaudoin JJ (2002) J Mater Sci Lett 21:1773
19. Ganesh I, Srinivas B, Johnson R, Saha BP, Mahajan YR (2001) Brit Ceram Trans 101:247
20. Bose S, Banerjee A (2004) J Am Ceram Soc 87:487
21. Prabhakaran K, Gokhale NM, Sharma SC, Lal R (2005) Ceram Int 31:327